On the Coupling Mechanism of a 780 nm Femtosecond Laser with Biphenyl, Diphenylmethane, and Diphenylethane

Richard Billotto and Robert J. Levis*,†

Department of Chemistry, Wayne State University, Detroit, Michigan 48202

Received: May 20, 1999; In Final Form: August 6, 1999

The coupling mechanism between an intense ($\sim 10^{13}$ W cm^{-2}, 780 nm) near-infrared radiation field of duration 125 fs with molecules containing 12−28 atoms is considered in this article. The time-of-flight mass spectra are reported for the molecules benzene (C_6H_6), biphenyl ($C_{12}H_{10}$), diphenylmethane ($C_{13}H_{12}$), and diphenylethane ($C_{14}H_{14}$). The ionization of these molecules is compared with the predictions of a quasistatic tunneling model giving experimental/calculated yields for benzene, biphenyl, diphenylmethane, and diphenylethane of 1:1, 27:257, 59:113, and 134:467, respectively. The model correctly predicts the order of relative ion yields: benzene < biphenyl < diphenylethane. The ionization probabilities are not correlated with those predicted by the Ammosov−Delone−Krainov (ADK) model. The ADK model predicts relative probabilities of 1 (benzene), 11.6 (biphenyl), 3.4 (diphenylmethane), 1.5 (diphenylethane) at a field strength of 1.2 V Å^{-1}. In addition, comparison of the Keldysh adiabaticity parameter, γ, to the structure-based adiabaticity parameter, $\gamma(\psi)$, at 1 V Å^{-1} returns ratios for $\gamma(\psi)/\gamma$ of 0.68, 0.35, 0.42, and 0.29 for benzene, biphenyl, diphenylmethane, and diphenylethane. These ratios suggest that tunneling ionization occurs at a lower intensity than that predicted by the Keldysh adiabaticity parameter.

1. Introduction

The interaction of gas-phase species, i.e., atoms, molecules, and clusters, with radiation of intensity exceeding 10^{13} W cm^{-2} is a complex process. In these intense fields, atoms and molecules have been observed to undergo massive Stark shifting, above threshold ionization (ATI),[1] as well as high harmonic generation (HHG).[2] In the case of molecules, energy may also couple into the nuclear modes of rotation, vibration, and dissociation, resulting in more complicated dynamics than atoms. Lower intensity, resonant, multiphoton ionization−dissociation investigations reveal that molecular ion formation competes with molecular dissociation as the pulse duration is decreased from nanosecond to picosecond duration.[3] At the higher intensities ($>10^{13}$ W cm^{-2}), molecules can undergo bond softening[1] or laser-induced stabilization[4] due to the high electric fields, and this leads to dissociation. This photochemistry arises from the motion of the vibrational wave packet along dressed molecular potential surfaces in the intense laser field. Such effects must be considered because the photon densities can be very large, $\sim 6 \times 10^8$ photons per cubic wavelength at 10^{13} W cm^{-2} and 780 nm. These effects serve to complicate the application of atomic models of intense field ionization to molecules. Here, we demonstrate that such models do not even qualitatively reproduce the ionization trends for the polyatomic molecules. We show that the ionization trends are consistent with a structure-based model and suggest possible mechanisms for radiation−molecule coupling based on this model.

To fully understand the molecular processes induced by intense radiation pulses, the time-dependent Schrödinger equation must be solved. Numerical, time-dependent[5] treatments have been performed to determine ionization rates and dissociation energies with some success. Time-dependent quantum calculations cannot be performed on complex molecules interacting with strong field radiation in or above the multiphoton limit, hence only the simplest molecules, (H_2^+),[6] (H_3^{2+}),[7] (H_4^{3+}),[7,8] (H_4^{2+}),[7,8] and, (H_2)[8] have been the subject of such calculations. Simplified models considering only portions of the Hamiltonian have been developed for more complex systems employing the single active electron[9] approach in the interest of obtaining timely and informative results. To develop these simplified pictures, the operative coupling may be viewed in one of two limits. In one limit, high photon densities may drive coherent multiphoton absorption processes where the atom or molecule can absorb photons simultaneously, e.g., a sufficient number of photons to produce nonresonant ionization. In the other limit, classical behavior may be conveyed to the laser−molecule (atom) interaction when photon densities much greater than 1 photon per cubic wavelength are employed.[10] In this case, the system may ionize through tunnel ionization (TI) or barrier suppression processes. An ongoing question in developing models to predict atomic and molecular behavior in the presence of high-intensity radiation centers on whether the coupling can be viewed as a multiphoton process or a field-induced process. While simple models may be employed to calculate ionization rates in the case of tunneling, no such calculations are possible at the present for high order MPI processes in polyatomic molecules.

A classical model used to predict the interaction mechanism in the MPI or TI limit was first proposed by Keldysh in 1964.[11] In this model, the ionization event is modeled by superposing an external field on a zero-range potential modeling the atom. This superposition results in a barrier through which an electron can tunnel. Keldysh introduces the adiabaticity parameter, γ, to define the regimes of TI ($\gamma \ll 1$) and MPI ($\gamma \gg 1$). Calculations using the zero-range model for molecules with IP between 8 and 16 eV interacting with 780 nm radiation in the range $10^{13}-10^{14}$ W cm^{-2} return an adiabaticity parameter in

* To whom correspondence should be addressed.
† Camille Dreyfus Teacher Scholar and Sloan Fellow.

10.1021/jp991663+ CCC: $18.00
Published on Web 09/28/1999

the range 2−5, suggesting MPI. The rare-gas atoms and their high charge states yield adiabaticity parameters in the range 1−8 using 248 nm laser radiation in the intensity range 10^{13}−10^{16} W cm^{-2}, also suggesting MPI. It is interesting that using a UV photon the experimental ionization thresholds for the various charge states are in agreement with several tunneling ionization models.[12] This should not be too surprising, however, because these Keldysh parameters are not much greater than 1. Recent experimental and theoretical studies have suggested that electronic delocalization is an important factor in the ionization of molecules.[13] These studies emphasize that with greater electronic delocalization there is a greater probability for field ionization as observed in the series cyclohexane, benzene, and 1,3,5-hexatriene. Here, the ionization probability increases monotonically as the extent of delocalization increases. This laboratory has developed a model[14] similar to the Keldysh model to account for the effect of the structure of the molecule on the ionization process. In this model, the zero-range potential is replaced with a more realistic one-dimensional potential based on the molecular wave function. A structure-based adiabaticity parameter is calculated in terms of this potential and has been denoted as $\gamma(\psi)$.

Investigations of the intense field ionization and dissociation of small molecules using 10.6 μm radiation have focused on measurement of the ion yield as a function of laser power density. At 10.6 μm, molecules including H_2,[15] N_2,[15] O_2,[15] CO,[15] HCl,[16] NO,[15] CO_2,[15] and I_2[17] ionize in a manner consistent with tunnel ionization (TI). Investigations of molecular hydrogen[1] at wavelengths near 1 μm and intensities of up to 10^{14} W cm^{-2} attribute the ionization and dissociation to multiphoton ionization (MPI). Attempts to model the ionization of diatomic molecules[15,18] have drawn on the Ammosov, Delone, and Krainov (ADK)[19] formalism for atomic ionization and are in agreement with experiment.

Although the gross features of the ionization of atoms and diatomics are described by the Keldysh and ADK models, the double ionization rates for helium at ∼10^{14}−10^{15} W cm^{-2} are not well predicted. This is because these models assume a single active electron (SAE) approximation. The experimental rates for second ionization are much higher than the rates calculated using the SAE,[20] this is because the first ionizing electron influences the rate of ionization of the second electron in two ways. The ionizing electron can perturb the potential influencing the second electron in a "shake off" mechanism[21] and it can impart energy to the second electron via scattering.[22] However, two active electron calculations are extremely time-consuming for atomics even when one space dimension is used. Unfortunately, polyelectron, polyatomic molecule calculations will require much more computer time and memory to obtain useful results.

For molecules, there is an open question as to whether the coupling mechanism is multiphoton ionization, MPI,[23−25] or tunneling ionization, TI.[7,12,14,26,27] In those cases where MPI has been argued, the exciting photon is in resonance with an intermediate transition or the exciting photon is a UV photon allowing for low-order MPI (<3 photons to reach a resonant level or ionize). Kosmidis et al.[23] show the effect of resonance in the log−log plots of relative ion yield vs laser intensity. For example, using 375 nm, 90 fs pulses over the range ∼1.2 × 10^{10} to 1.2 × 10^{11} W cm^{-2}, the measured gradients (slopes) of nitromethane and its fragments are between 2 and 3. Using 750 nm pulses under the same conditions, the slopes are between 4 and 5.[23] This is consistent with resonant MPI where halving the energy of the absorbed photon requires doubling the number of photons absorbed. On the other hand, cases where tunnel ionization has been argued involve nonresonant photons or high order (>5 photons to reach a resonant level or ionize) processes. For example, experiments done at (∼1.0−3.8) × 10^{13} W cm^{-2} using 170 fs pulses centered at 780 nm are consistent with tunneling ionization.[13,14,26] Furthermore, the relative ionization rates of benzene, naphthalene, anthracene, 1,3,5-hexatriene, and cyclohexane, are well predicted by calculations based on a TI model.[13,28] Subsequent measurement of the photoelectron spectra of benzene, naphthalene, and anthracene are consistent with a transition from partial MPI to pure TI.[29] This suggests that a simple MPI process is not dominant in these molecules using the laser conditions outlined elsewhere.[26]

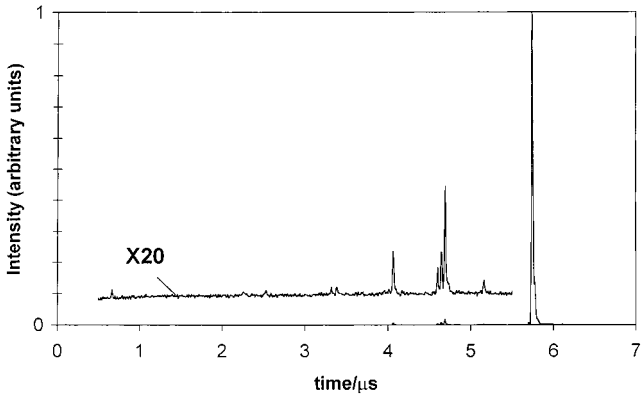

Figure 1. Time-of-flight mass spectrum of benzene at 4.8 × 10^{13} W cm^{-2}. The inset is a 20 times multiplication of the time region spanning 0.5−5.5 μs.

In this paper, we extend the investigation of the structure-based coupling model for intense laser−molecule interaction to more complex aromatic systems including, biphenyl, diphenylmethane, and diphenylethane. This series can be written as $C_6H_6(CH_2)_nC_6H_6$ where methylene groups are added between phenyl rings and $n = 0$ for biphenyl, 1 for diphenylmethane, and 2 for diphenylethane. In terms of the structure-based model, this modification changes the optimal one-dimensional potential energy surface and should be reflected in the experimental ionization probability as well as the relative ionization probabilities predicted by our model. In previous applications of the structure-based tunneling model, we have employed ab initio potential energy surfaces in order to determine optimal one-dimensional potentials for laser−molecule coupling. In this work, we use PM3 calculated geometries to simplify the determination of the optimum one-dimensional potential. We compare previously calculated tunneling probabilities using ab initio potential energy surfaces of benzene and naphthalene to the probabilities obtained using PM3 geometries. Finally, we calculate zero-range and structure-based adiabaticity parameters to provide some indication of the coupling mechanism.

2. Experimental Section

2.1. Femtosecond Laser. The femtosecond laser used in this investigation has been described previously.[26] Briefly, the output of a Coherent Mira laser was stretched, regeneratively amplified, and recompressed to deliver amplified pulses with energies of ∼500 mJ and autocorrelated temporal pulse widths (fwhm) of ∼125 fs. The estimated intensity for a focused (50 mm radius) pulse at maximum intensity is 5.1 × 10^{13} W cm^{-2}. This pulse intensity corresponds to a maximum field strength of 1.94 V Å^{-1}. Studies of ion production at varying laser intensities were performed to determine the relationship between ionization/

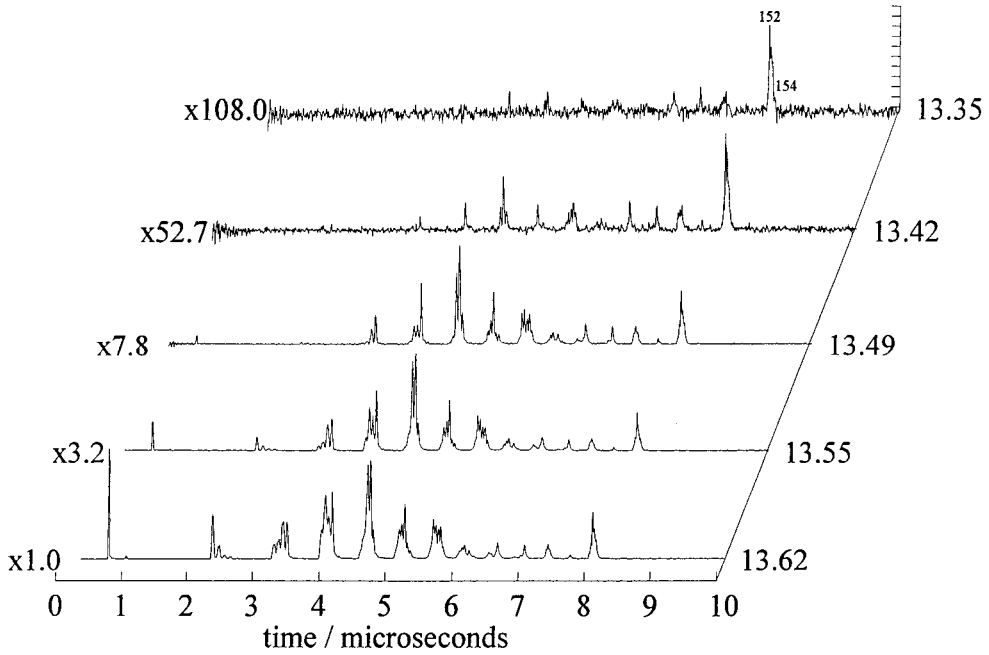

Figure 2. Time-of-flight mass spectra for biphenyl as a function of 780 nm laser intensities. The value to the right of each spectrum is the logarithm of the laser intensity.

dissociation and laser intensity. The intensity was attenuated using glass slides with a 5% reduction in pulse intensity per slide. This gave a range of intensities from $10^{13.2-13.7}$ W cm^{-2} (1.09−1.94 V Å^{-1}). Threshold fragmentation spectra of benzene were used to calibrate the intensity. Benzene fragmentation was determined to occur at approximately 3.21×10^{13} W cm^{-2}. Using this calibration point, the intensities from one power study to the next could be matched. Matching intensities in this manner resulted in an uncertainty of the laser intensity of ≤5%. The relative ion yields will be affected by this error, but the qualitative relationship between the probabilities for ionization will remain (see the Discussion section). The orders for these processes are unaffected by this matching error.

2.2. Time-of-Flight Mass Spectrometer. The time-of-flight system used in this investigation has been described previously[30] and only a brief description will be presented here. This system employed a dual-slope extraction region to enhance mass resolution. Positive ions were extracted through a 1900 V potential into a 12 cm field-free region. The detector consisted of a chevron-stacked dual microchannel plate assembly, and signals were averaged and stored on a LeCroy 7200 A digital oscilloscope. Data were downloaded to a PC for data storage and analysis. Benzene and diphenylmethane are liquids at room temperature and were introduced into the chamber via a pulsed nozzle that was not in line of sight with the ionization region of the spectrometer. Consequently, a static, thermalized, room-temperature gas was the state of these analytes in the experiment. Biphenyl and diphenylethane are solids at room temperature and were introduced by placing the sample in a small Eppendorf tube with a hole in it and allowed to effuse into the vacuum chamber. The samples were obtained from the Aldrich Chemical Co. and used as supplied by the manufacturer.

3. Results

To elucidate the mechanisms of ionization and dissociation, mass spectra were recorded as a function of laser intensity. As observed in previous investigations,[26,31] benzene gives predominantly the radical cation upon interaction with the photon field. Benzene does show some fragmentation at the highest intensities corresponding to $C_3H_x^+$, $C_4H_x^+$, $C_5H_x^+$, and H^+ (see Figure 1). At lower laser intensities, no fragmentation was observed.

Biphenyl, diphenylmethane, and diphenylethane mass spectra are plotted as a function of laser intensity in Figures 2−4, respectively. The laser intensity ranges from 2.24 to 4.17×10^{13} W cm^{-2} (i.e., $10^{13.35-10^{13.62}}$ W cm^{-2}). This range of intensities does not encompass the entire range of intensities employed for each molecule; this is the common range over which all molecules have been irradiated. As shown in Figure 2, biphenyl exhibits an extensive amount of dissociation with the $C_{1-6}H_x^+$ ($x = 0-5$) and H^+ fragments dominating the spectra at the highest laser intensities. As the intensity of the excitation laser is reduced, so also is the dissociation; the dissociation is attenuated to the extent that the spectra show almost no fragmentation relative to the parent ion at the lowest intensities. Diphenylmethane, on the other hand, produces the parent ion as the major species in the laser field throughout the range of intensities employed as illustrated in Figure 3. Again, at the lowest laser intensities, the spectra display predominantly parent ion; at the appearance intensity (not shown), the parent ion is the only peak observed in the mass spectrum. Note that, for both biphenyl and diphenylmethane, as the carbon number of the fragment species increases, the distribution of hydrogens shifts toward a larger number. For example, the distribution of hydrogens for C_2 is 0−4 and that for C_{12} in biphenyl is 6−10. As an example of an extreme case of fragmentation in this series, diphenylethane dissociates to give $C_7H_7^+$ as the predominant species with very little parent ion appearing in the spectra (see Figure 4). The molecule also dissociates into the fragments $C_{1-6}H_x$ ($x = 0-5$). Also, note that very little dissociation results in fragment ions of $C_{8-13}H_x^+$. At the appearance intensity, the $C_7H_7^+$ is the only mass spectral peak.

4. Discussion

4.1. Ionization Order. The relationship between the ion yield and the laser intensity may provide useful information regarding the coupling mechanism of the near-IR radiation field with

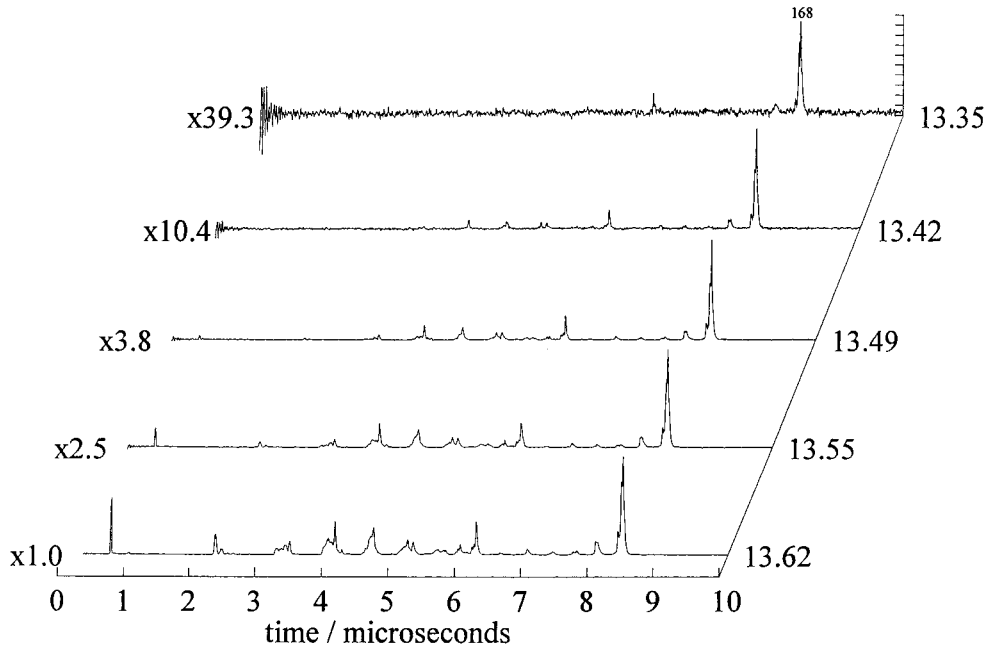

Figure 3. Time-of-flight mass spectrum for diphenylmethane as a function of 780 nm laser intensities. The value to the right of each spectrum is the logarithm of the laser intensity.

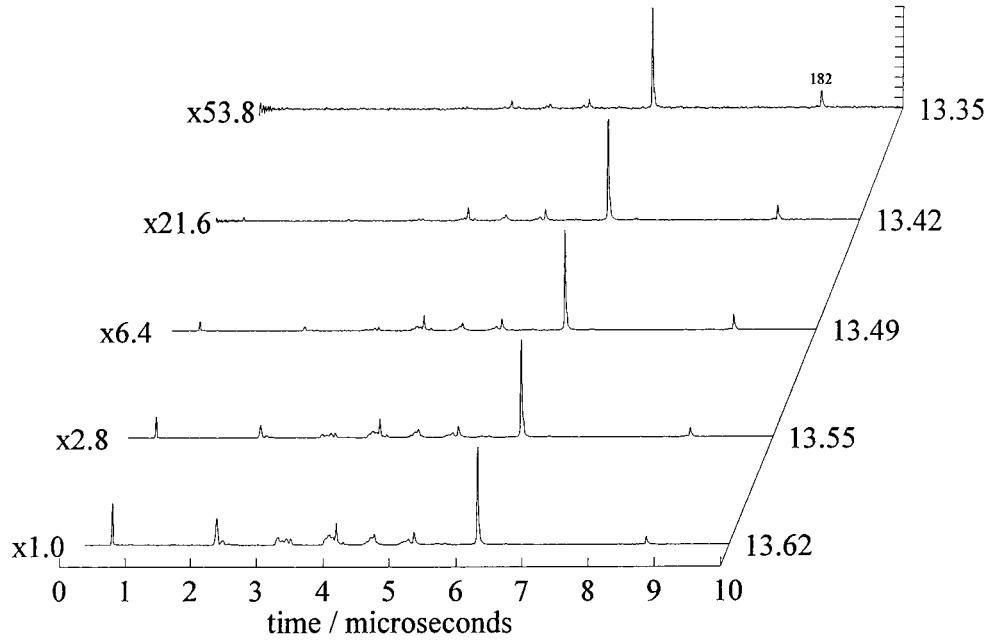

Figure 4. Time-of-flight mass spectrum for diphenylethane as a function of 780 nm laser intensities. The value to the right of each spectrum is the logarithm of the laser intensity.

polyatomic molecules. For example, the order of an MPI process is determined by the slope of a log−log plot of the ion intensity vs laser intensity. The order is generally equal to the minimum number of photons necessary to reach an allowed excited state or ionization level of the system. To generate such a plot, the following data processing routine is followed. The ion intensities in the TOF spectra were integrated for the molecules benzene, biphenyl, diphenylmethane, and diphenylethane over the range of laser intensities investigated. The integrated counts were corrected for pressure and laser intensity for direct comparison. The logarithm of these yields was plotted against the logarithm of the laser intensity. A linear least-squares fit to each data set is shown in Figure 5. The apparent order obtained from this slope is recorded in Table 1. (Note: naphthalene has been included in the table for the purpose of comparison.) The table shows that each of the apparent orders are approximately 8 or slightly greater (i.e., biphenyl). Given a 1.59 eV photon (780 nm), this order is two to four photons above the IP for these molecules. Extra photon absorption is not consistent with a simple MPI mechanism because one would expect ionization to occur via the lowest order process, ≤ 6 photons for the molecules considered here. Extra photon absorption may imply an ATI mechanism for ionization. However, as pointed out by Muller et al.,[32] extra photon absorption by ionized electrons in the ATI step is distinct from the ionization step. Thus, the observation of ATI peaks in photoelectron spectra need not indicate anything about the ionization process itself. With this in mind, one must consider extra photon absorption in the ionization step alone in order to understand the higher than expected orders observed in our laboratory. It is important to

TABLE 1: Experimental and Calculated Molecular Properties Pertinent to This Investigation

	benzene	naphthalene	biphenyl	diphenylmethane	diphenylethane
IP (vertical) (eV)	9.24	8.15	8.37	8.81	9.1
IP + U_p (eV)	11.41	10.3	10.11	10.71	10.86
order, total ion yield	8.2	8.5	9.0	7.7	7.8
expected order, MPI	5.8 (6)	5.1 (6)	5.0 (5)	5.4 (6)	5.5 (6)
predicted order, IP + U_p (U_p = 2.16 eV)	7.2	6.5	6.4	6.7	6.8
PM3 longest interatomic distance + 2.68a_0	6.39 Å 12.1 bohr	8.62 Å 16.3 bohr	10.65 Å 20.13 bohr	10.33 Å 19.52 bohr	12.80 Å 24.19 bohr
$\sigma_{rel,780}$ total	1.00	20[a]	27	59	134
$\sigma_{rel,ADK}$ [at 1.2 V Å^{-1}]	1.00	21.3	11.6	3.4	1.5
$\sigma_{rel,S-B}$ [at 1.2 V Å^{-1}]	1	68	257	113	467
$\epsilon_{rel,260}$[b]	1	19.8	66.0	2.82	2.37
no. of atoms	12	18	22	25	28
γ at 1.0 V Å^{-1}	2.48	2.32	2.36	2.42	2.46
$\gamma(\psi)$ at 1.0 V Å^{-1}	1.67	1.15	0.91	1.05	0.78

[a] Obtained in ref 26. [b] *UV Atlas of Organic Compounds*; Perkampus, H.H., Ed.; Butterworths, London, 1966−1971.

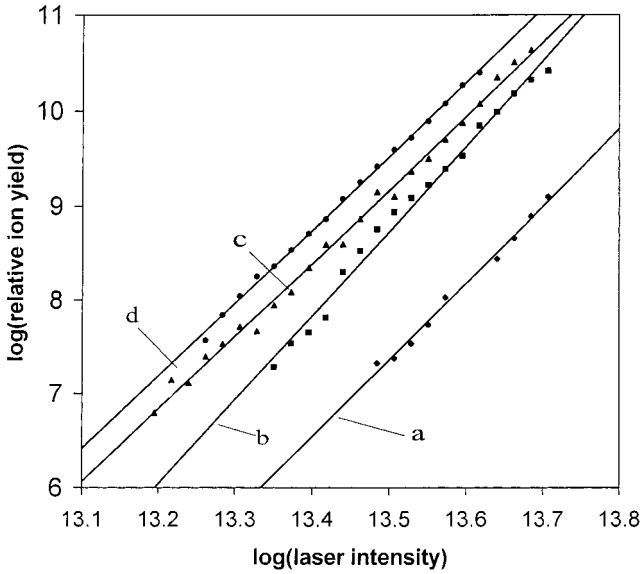

Figure 5. Plot of the logarithm of the integrated total ion yield as a function of the logarithm of ionizing laser power using 780 nm light, 125 fs duration for (a) benzene, (b) biphenyl, (c) diphenylmethane and, (d) diphenylethane.

note that the ionization order may have no meaning, in the MPI sense, if the ionization mechanism occurs via tunneling. This is because in the tunneling model (see Gibson et al.[33]) the only laser parameter taken into account is the electric field strength (or equivalently the laser intensity). Frequency is not taken into account and therefore determining the number of "absorbed" photons may be irrelevant.

An alternative explanation for the excess order, in the case of MPI, might be the increase in the IP due to the high electric field strength. In an intense laser field, the ionization level is shifted by an amount equal to the ponderomotive potential.[34] One calculates the ponderomotive potential using the following equation:

$$U_p = \frac{e^2 E_0^{\,2}}{4 m_e \omega^2} \qquad (1)$$

where E_0 is the electromagnetic field strength, e is the electron charge, m_e is the electron mass, and ω is the laser frequency. The ponderomotive shift is 2.16 eV at 3.8 × 10^{13} W cm^{-2} for 780 nm light. This accounts for about one and a half photons above the unperturbed IP. We may reconcile the apparent order for the total ion yield of benzene by taking into account the ponderomotive shift in the IP, as benzene requires two photons above the IP. However, this is not the case for the remaining molecules as shown in Table 1. From the apparent orders for the total ion yield of diphenylmethane, diphenylethane, and naphthalene, approximately three photons are absorbed above the IP and biphenyl absorbs four photons above the IP. This leaves one to two photons unaccounted for in these molecules. Furthermore, the ponderomotive shift in the IP should increase with increase in laser intensity and so should the ionization order. However, the slopes for these molecules are linear over the range of intensities considered here. In addition to the possibility of tunneling, there are many potential explanations for the higher than expected slope. Experimentally, these include systematic error in pulse duration or pulse energy measurements and difficulty in obtaining a homogeneous laser beam profile.

4.2. Relative Ionization Probability. The log−log plots can be used to compare the relative ion yields of the molecules. The relative ion yields indicate an ordering of the molecular ionization probabilities. One important assumption in this comparison is that the orders for each of the molecules be nearly equal, as is the case for this series. The relative ion yields are recorded in Table 1 at 3.8 × 10^{13} W cm^{-2}. Over the range of intensities studied, the ion yield increases across the series of molecules benzene < naphthalene < biphenyl < diphenylmethane < diphenylethane. The ionization trend is correlated with the number of atoms contained in the molecule (see Table 1). There is no correlation between ionization probability and ionization potential, as would be expected in the ADK model.[19,35] In the ADK model the tunnel probability is defined as

$$w = \left(\frac{3E_0}{\pi F_{IP}}\right)^{1/2}\left(\frac{2F_{IP}}{E_0}\right)^{2} n|C_{n^*l^*}|^2\left(\frac{E_0}{2F_{IP}}\right)^{m+1} f(l^*,m) \exp\left[\frac{-2F_{IP}}{3E_0}\right] \qquad (2)$$

where $F_{IP} = (2IP)^{3/2}$, $n = Z(2IP)^{-1/2}$, IP is the ionization potential, Z is the resulting charge, E_0 is the amplitude of the electric field, and n^*, l^*, and m are the effective principal, effective orbital, and magnetic quantum numbers, respectively. The remainder of the constants are defined following ref 35. As shown in Table 1, the relative ADK probabilities predict a descending order of relative ionization probabilities for biphenyl, diphenylmethane, and diphenylethane, consistent with their increasing ionization potentials. The measured relative ionization probabilities are not in agreement with the prediction of the

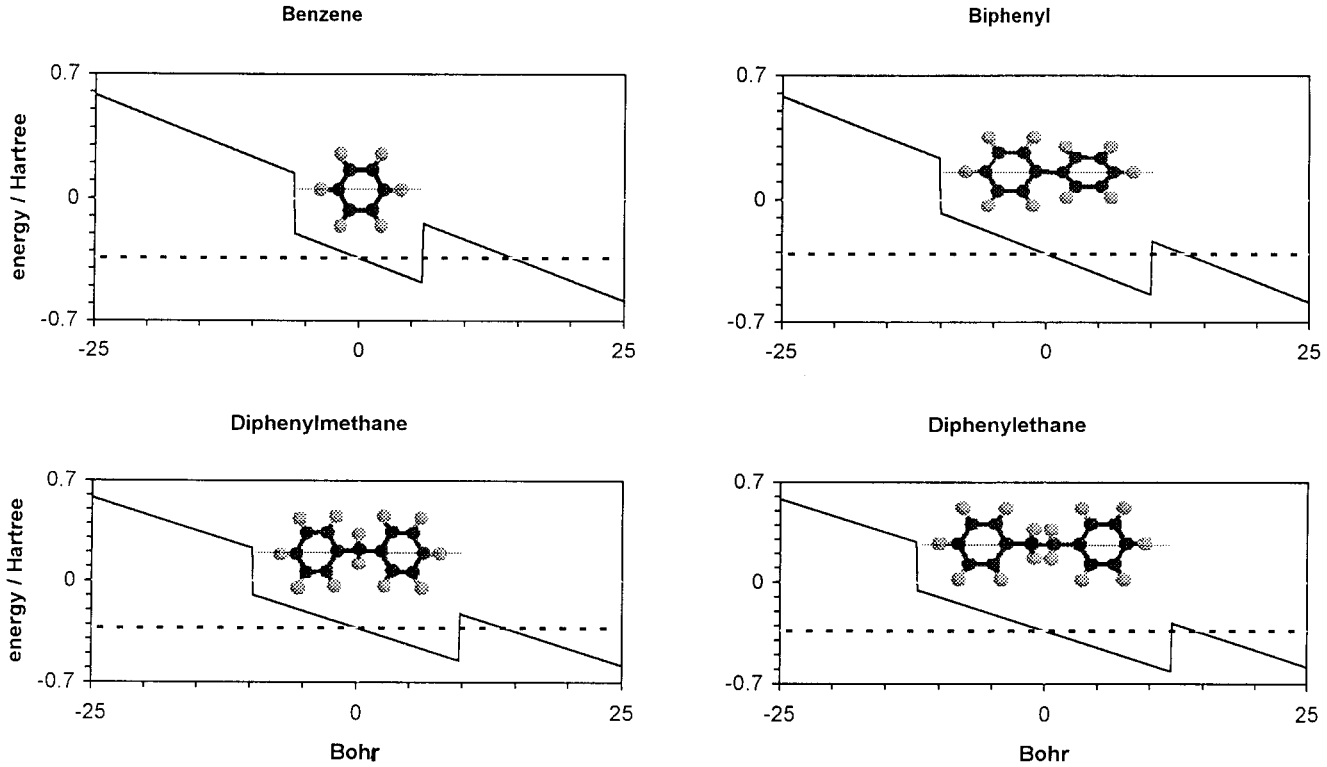

Figure 6. schematic of the one-dimensional models for field ionization for the molecules investigated. The rectangular wells depict a given molecular potential with a height of IP and a length as defined in the text. An electric field of 1.2 V Å^{-1} is superimposed on each rectangular well.

ADK model. This suggests some role of electronic delocalization in the ionization rate for these molecules. The relative ionization probabilities can be quantitatively predicted by the model outlined subsequently.

To model the ionization process, a formalism has been developed for calculating relative ionization rates based on a static field excitation.[13] This formalism seeks to account for the fact that polyatomic molecules have delocalized electronic orbitals that are not well described by zero-range or Coulomb potentials. To account for the extended structure of polyatomic molecules, we determine a one-dimensional characteristic length for interaction with the laser electric field. While there are an infinite number of different one-dimensional potentials in a polyatomic wave function, there is only one optimal potential. The optimal one-dimensional potential has the greatest distance between classical turning points at the ionization potential of the neutral. The field−molecule interaction is then approximated by superimposing the electric field of the intense laser upon a representation of this one-dimensional potential.

In previous work,[13,28] the input for determining the optimal one-dimensional molecular potential is usually derived from an ab initio calculation of the molecular wave function over all space. From this, the one-dimensional potential that has the greatest distance between classical turning points at the ionization potential is determined. The length between these classical turning points defines the characteristic length of the molecule. This is the length available for coupling with the electric field of the laser. In the model, the characteristic length is employed as the width of a rectangular potential used to approximate the molecule's electrostatic potential energy surface. The height of the well corresponds to the molecule's ionization potential. The electric field of the laser is then superimposed on this rectangular well. The result of this superposition is a barrier through which the electron may tunnel. The WKB approximation for tunneling through a barrier is then used to calculate the tunnel probability in atomic units,

$$T = \exp[-2 \int_{r_1}^{r_2} \{2[\mathrm{IP} - V(r)]\}^{1/2} \, \mathrm{d}r] \qquad (3)$$

where T is the transmission coefficient for barrier penetration, IP is the ionization potential, $V(r)$ is the molecular potential with the electric field superimposed upon it, and r_1 and r_2 are the classical turning points defined by the molecular potential and molecular field. The transmission coefficient is a measure of the probability for ionization. In previous work, application of the WKB equation was used to predict the relative ionization probabilities for the series: benzene (C_6H_6), 1,3,5-hexatriene (C_6H_8), cyclohexane (C_6H_{12}), and *n*-hexane (C_6H_{14});[13] benzene, naphthalene, and anthracene;[29] and acetylene, ethylene, and ethane.[36] To calculate the characteristic length of the molecular potential, it is assumed that the conformation which is lowest in energy is the dominant gas-phase species. For example, only the anti conformation of *n*-hexane (i.e., the most linear) was assumed to contribute significantly to the total ionization probability.[13] In the structure-based model, the least compact configuration will contribute most significantly to the tunnel ionization rate. This is because the largest linear dimension usually provides the largest potential drop across the molecule resulting in the greatest barrier suppression. The application of this model to the above listed molecules agreed well with experimentally measured relative ionization rates.

In this investigation, the semiempirical PM3-based method[37] is employed to calculate the nuclear geometry to determine the characteristic length. Previously ab initio methods have been employed for the determination of the characteristic length by defining the largest distance between classical turning points in a molecule. In the PM3-based method, the characteristic length is taken as the sum of the distance between the two most distant hydrogen atoms in the molecule and a constant equal to 2.68 bohr (see Figure 6). The constant is added to account for

extension of the classical electronic turning points beyond the distance defined by the nuclear positions. The value of 2.68 bohr is determined by taking the average difference between the length defined by the classical turning points on the electrostatic potential energy surface and that defined by the nuclear position for the most distant hydrogen atoms in benzene, naphthalene, and anthracene. It is reasonable to use these aromatic molecules to calibrate the PM3-based method for biphenyl, diphenylmethane, and diphenylethane because these molecules also possess aromatic character. The internuclear distance between the two furthest hydrogen atoms can be simply determined from the geometry optimized configuration at the PM3 level. To test the effect of this approximation, we compare the relative ionization probability predicted for benzene and naphthalene using the two methods. The relative ionization probability calculated using the PM3-based method for naphthalene is higher than that reported in a previous ab initio based calculation as noted Table 1. We attribute this to two factors. First, in the previous ab initio calculations a characteristic length of ~15 bohr was used, and in this work the characteristic length obtained is 15.6 bohr. Second, a calculated value of 8.575 eV was used for the vertical ionization potential of naphthalene in the ab initio study, and here the experimental vertical IP of 8.15 eV is used. It is reasonable that a shorter box length and higher ionization potential will result in a lower tunnel rate for the electron in the ab initio based method. We conclude that the PM3-based method is a reasonable means to obtain the characteristic length given the facile implementation of the calculation.

For biphenyl, diphenylmethane, and diphenylethane, the lowest energy nuclear conformation calculated at the PM3 level was selected for use in the structure-based tunnel calculation. The one-dimensional potentials resulting from the superposition of the approximate rectangular potentials with a static electric field of 1.2 V $Å^{-1}$ are shown for benzene, biphenyl, diphenylmethane, and diphenylethane in Figure 6. The box length, IP, and calculated relative rate are included in Table 1 for each molecule. The calculated rates predict the ordering of the probability for ionization: benzene (exptl, 1.00; calcd, 1.00) < naphthalene (exptl, 20; calcd, 68) < biphenyl (exptl, 27; calcd, 257) < diphenylethane (exptl, 134; calcd, 467). We conclude that the model reproduces the relative ionization probabilities for these molecules reasonably well. However, we must note that the calculated length of diphenylmethane is shorter than the length for biphenyl. This along with a higher IP gives diphenylmethane a smaller calculated transmission coefficient than biphenyl. This is in apparent contradiction to the experimental data where diphenylmethane has a higher ionization probability (exptl, 59; calcd, 113) than biphenyl.

Several possibilities exist as to why the model does not predict the relative ordering for diphenylmethane in this series. The first hypothesis centers on a channeling of excitation energy into nuclear modes during the excitation time scale. The structure-based tunnel ionization model takes no account of channeling of energy into nuclear modes and dissociation. However, in the field-induced excitation process, there will be a competition between energy deposition into nuclear modes and electronic excitation. It has been proposed previously[13,31] that, in the cases where dissociation begins to dominate the mass spectrum, the calculated ionization probability overestimates the experimentally measured ionization probability. For instance, in the case of a comparison of a series of alkyl-substituted benzene molecules, the species that had the highest dissociation probability (*n*-propylbenzene) also gave the lowest ionization

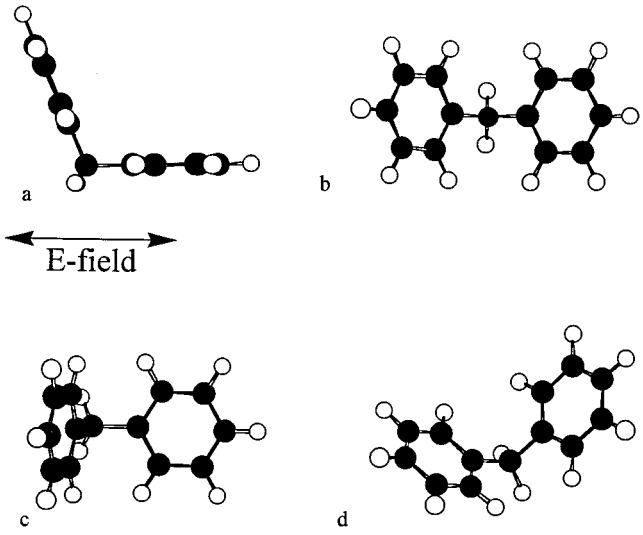

Figure 7. A selection of molecular orientations of diphenylmethane relative to the electric field vector, *E*.

yield in comparison to the expected yield.[31] Diphenylmethane may have a higher relative ionization probability than biphenyl because it actually has a lower cross section for ionization/dissociation. Note that in the cases of biphenyl and diphenylethane, the degree of dissociation is such that the parent ion peak is not the largest peak in the mass spectrum. In these cases, fragmentation/ionization dominates molecular ionization. One might anticipate that a large fraction of energy will channel into dissociation at the expense of ionization for these two molecules. Diphenylethane apparently has a larger ionization cross section than diphenylmethane by virtue of its characteristic length, thus diphenylethane's relative ionization cross section is largest despite its increased fragmentation. The dissociation/ionization of benzene, biphenyl, diphenylmethane, and diphenylethane will be the subject of a later publication.[38]

Another hypothesis as to why the model may not predict the relative ionization rate for diphenylmethane concerns the lack of statistical sampling of all contributing molecular orientations in the electric field. The model includes only one orientation for calculating the rate, that giving the largest distance between classical turning points. Other orientations will contribute to the ionization pathway, especially for molecules that are inherently nonplanar such as diphenylmethane. The largest cross section occurs when the molecule is aligned such that its characteristic length is aligned with the electric field vector giving optimum coupling. For planar or nearly planar molecules, it is relatively easy to determine the optimum geometry for coupling between the molecule and the field. This geometry exists when the direction of the electric field vector is parallel to the plane of the molecule and pointed along the optimal one-dimensional potential energy surface. For example, in the case of benzene, there should be negligible probability for tunneling when the electric field vector perpendicular to the plane of the molecule in comparison to parallel orientations. Therefore, this contribution to the total ion yield of benzene can be neglected. Biphenyl and diphenylethane can take on a configuration that will allow the phenyl moieties to be nearly parallel. On the other hand, diphenylmethane cannot have both rings "coplanar" (see Figure 7a) because of the tetrahedral structure of the methylene carbon. (There is a configuration that has the rings nearly coplanar, but it is highly energetic, approximately 0.87 eV greater than the geometry used to determine the box length for the tunneling calculation.) Although coupling into a single molecule may be greatest when the planar configuration is

aligned optimally with the field, in an ensemble, a large number of nonplanar orientations with some degree of coupling may yield a larger total ion current despite a lower ionization probability. Some of the orientations for diphenylmethane are shown in Figure 7. Consider what would happen if diphenylmethane had its greatest coupling when one ring has its vector aligned with the field (see Figure 7a). If this were the only orientation which contributed to ion current the diphenylmethane relative ion yield would be expected to be within an order of magnitude of benzene; it is not. Clearly, other orientations can couple with the field (see Figure 7b−d), including the one with the largest cross section for interaction (see Figure 7b).

While the calculated relative ion yield for biphenyl is ∼6.7 times greater than that for naphthalene, the experimental values are quite close ($\sigma_{rel,biphenyl}/\sigma_{rel,naphthalene} \cong 1.5$) at 3.8×10^{13} W cm^{-2} (see Table 1). This is further evidence for the fact that dissociation may reduce the observed ionization yield (for comparison see Figure 5 in ref 26). In addition, the model does not include dipole moments, polarizabilities, hyperpolarizabilities, or electron correlation; these and other electronic factors may become important in predicting tunneling rates in molecules. An extension of the model, which includes these factors along with orientation, should provide a more accurate means to calculate tunneling rates. In the case of electron correlation, the effects of double excitation on the single ionization rates of He and Mg atoms have been investigated.[39] In He, the first double excitation is well above the ground-state energy (>40 eV) and the influence on the single ionization rate is negligible. Mg, on the other hand, has the first double excitation energy at ∼8.4 eV. Under the appropriate laser intensity (∼10^{14} W cm^{-2}) and frequency conditions (resonance) double excitations reduce the rate (and probability) of single ionization. In sequential ionization, one electron ionizes in a core with reduced screening due to the second excited electron. It is probable that double excitations occur in molecules (their double excitation energies are relatively low) and may have a similar effect on the ionization rate. To observe the decreased ionization probability, due to double excitations, the double excitation states should be relatively long lived. A decrease in the time-of-flight mass resolution, ($t/\Delta t$), of the parent ion may be observed when the laser is tuned to a double excitation resonance. This is because at resonance a very slow ionization rate will yield ions over a long period of time. However, in the presence of Stark and ponderomotive energy level shifting it is hard to predict which molecules will be subject to double excitation using 780 nm. The decreased ionization rate may allow for energy redistribution throughout the molecule leading to increased dissociation. In addition, double excitations may explain the higher than expected ionization orders for the molecules studied here. The second excitation may compete with the first ionization. In a high-intensity femtosecond laser pulse, the doubly excited neutral may absorb additional photons above the IP to produce an elevated order and still ionize on the time scale of the laser pulse.

4.3. Coupling Mechanism. The importance of molecular and electronic structure is strongly suggested by the ability of the structure-based tunneling model in predicting the relative ion yields for the molecules benzene, naphthalene, biphenyl, diphenylmethane, and diphenylethane. This also suggests that models, such as the Keldysh adiabaticity parameter, should account for molecular and electronic structure. Thus, a structure-based adiabaticity parameter,[14] $\gamma(\psi)$, may be a more accurate descriptor of the coupling mechanism than a zero-range parameter. For instance, using the Keldysh adiabaticity parameter at 1.0 V Å^{-1}, the values 2.30, 2.38, and 2.40 are obtained for biphenyl, diphenylmethane, and diphenylethane, respectively (see Table 1). These values are in an intermediate region and suggest a multiphoton component to the ionization mechanism. On the other hand, if the molecular adiabaticity parameter, $\gamma(\psi)$, is calculated as prescribed by DeWitt and Levis[14] the values returned at 1.0 V Å^{-1} for each molecule are biphenyl, 0.81, diphenylmethane, 0.99, and diphenylethane, 0.68. Thus, these molecules are actually further into the tunneling regime than would be predicted by the Keldysh parameter.

From this series, we can also determine whether simple scaling laws exist for predicting relative ionization probability. For instance, the intense laser ionization probabilities might be predicted by the sum of the ionization probabilities for individual chromophores within a molecule. To make this determination, the relative ionization yields for benzene and diphenylethane are compared. In this model, we would expect diphenylethane to have an ionization probability approximately twice that of benzene. This is because the phenyl chromophores in diphenylethane are sufficiently far apart as to be decoupled in terms of the linear absorption probability. This decoupling is suggested by the $\epsilon_{rel,260}$ (see Table 1) for benzene and diphenylethane which is approximately 1:2. The measured relative cross sections for intense laser ionization are 1:134 for benzene/diphenylethane, suggesting some degree of coupling into the entire molecule as in the structure-based model. The effect of decoupled individual chromophores within one molecule could also result in multiple ionization. However, as pointed out earlier, there is no evidence for multiple charging.

Finally, we would like to consider whether a resonant multiphoton model might be invoked to rationalize the experiments. If we assume that a resonance exists approximately 4.77 eV above the ground electronic state, then the cross section for absorbing a 260 nm photon (3 × 780 nm) may correlate with the ionization probability and hence the observed ionization yield. The predicted ordering of the relative ion yields from the ϵ_{260} values is benzene < diphenylethane ≅ diphenylmethane ≪ biphenyl (see Table 1). There is no correlation between ϵ_{260} and measured ionization probabilities, suggesting that a multiphoton resonance mechanism is most probably inoperative for the ionization process of these molecules. In addition, it would require three 780 nm photons to reach a resonance of about 4.77 eV above the ground state, i.e., a (3 + 3) ionization process. If resonant MPI were the mechanism of ionization, the log−log plots should reveal a slope of 3. Again, the plots show slopes that are approximately equal to 8 or greater (see Table 1).

5. Conclusions

The use of the PM3-based one-dimensional potentials in constructing one-dimensional rectangular wells for the molecules biphenyl, diphenylmethane, and diphenylethane illustrate the ability of the structure-based tunneling model to predict relative ionization probabilities for intense near-infrared excitation. The structure-based tunneling model includes an element of molecular structure, the characteristic length, unlike zero-range and Coulomb models. Using the structure-based method to calculate relative ionization probabilities, we find experimental to calculated relative ionization cross sections of 1:1 for benzene, 68:20 for naphthalene, 257:27 for biphenyl, 113:59 for diphenylmethane, and 467:134 for diphenylethane. It has been shown that the relative ionization probabilities as calculated using the ADK model do not correlate with the experimental probabilities. A (3 + 3) resonant multiphoton ionization process is also not consistent with the measured slopes in log−log plots

of the ion yield dependence on the laser intensity for these molecules. Calculation of the molecular adiabaticity parameter, $\gamma(\psi)$, reveals that the onset of tunnel ionization occurs at lower intensities for the structure-based model than predicted by the Keldysh parameter. We conclude that the coupling between the intense 780 nm radiation pulse and biphenyl, diphenylmethane, and diphenylethane occurs via a field-mediated mechanism (such as tunneling or barrier suppression) rather than a multiphoton process. Finally, there is some correlation between decreased experimentally measured ionization probability with increasing fragmentation/ionization as was observed, for instance, in biphenyl whose measured relative ion yield is ~9.5 times lower than the relative ion yield predicted by the structure-based tunnel model.

Acknowledgment. We acknowledge Merrick DeWitt for numerous stimulating discussions and assistance with the calculations included in the table. We acknowledge the support of the National Science Foundation through a Young Investigator Award (R.J.L.). The support of the Sloan and Dreyfus Foundations is also greatly appreciated.

References and Notes

(1) Zavriyev, A.; Bucksbaum, P. H.; Muller, H. G.; Schumacher, D. W. *Phys. Rev. A* **1990**, *42*, 5500.

(2) Liang, Y.; Augst, S.; Chin, S. L.; Beudoin, Y.; Chaker, M. *J. Phys. B: At. Mol. Opt. Phys.* **1994**, *27*, 5119.

(3) Szaflarski, D. M.; El-Sayed, M. A. *J. Phys. Chem.* **1988**, *92*, 2234.

(4) Guisti-Suzor, A.; Mies, F. H. *Phys. Rev. Lett.* **1992**, *68*, 3869.

(5) Yu, H.; Zuo, T.; Bandrauk, A. D. *Phys. Rev. A* **1996**, *54*, 3290. Zuo, T.; Bandrauk, A. D. *Phys. Rev. A* **1995**, *52*, 1. Chelkowski, S.; Bandrauk, A. D. *J. Phys. B: At. Mol. Opt Phys.* **1995**, *28*, L1. Dietrich, P.; Corkum, P. B. *J. Chem. Phys.* **1992**, *97*, 3187. Thachuk, M.; Wardlaw, D. M. *J. Chem. Phys.* **1995**, *102*, 7462.

(6) Chelkowski, S.; Foisy, C.; Bandrauk, A. D. *Phys. Rev. A* **1998**, *57*, 1176.

(7) Yu, H.; Zuo, T.; Bandrauk, A. D. *J. Phys. B: At. Mol. Opt.* **1998**, *31*, 1533.

(8) Yu, H.; Bandrauk, A. D. *Phys. Rev. A* **1997**, *56*, 685.

(9) Krause, J. L.; Schafer, K. J.; Kulander, K. C. *Phys. Rev. A* **1992**, *45*, 4998. Krause, J. L.; Schafer, K. J.; Kulander, K. C. *Phys. Rev. Lett.* **1992**, *68*, 3535. Xu, H.; Tang, X.; Lambropoulos, P. *Phys. Rev. A* **1992**, *46*, R2225.

(10) Sakurai, J. J. *Advanced Quantum Mechanics*; Addison-Wesley: Reading, MA, 1967.

(11) Keldysh, L. V. *Sov. Phys. JETP* **1965**, *20*, 1370.

(12) Gibson, G.; Luk, T. S.; Rhodes, C. K. *Phys. Rev. A* **1990**, *41*, 5049.

(13) DeWitt, M. J.; Levis, R. J. *J. Chem. Phys.* **1998**, *108*, 7045.

(14) DeWitt, M. J.; Levis, R. J. *J. Chem. Phys*. **1998**, *108*, 7739.

(15) Walsh, T. D. G.; Ilkov, F. A.; Decker, J. E.; Chin, S. L. *J. Phys. B: At. Mol. Opt. Phys.* **1994**, *27*, 3767.

(16) Dietrich, P.; Corkum, P. B. *J. Chem. Phys.* **1992**, *97*, 3187.

(17) Dietrich, P.; Strickland, D. T.; Laberge, M.; Corkum, P. B. *Phys. Rev. A.* **1993**, *47*, 2305.

(18) Chin, S. L.; Liang, Y.; Decker, J. E.; Ilkov F. A.; Ammosov, M. V. *J. Phys. B: At. Mol. Opt. Phys.* **1992**, *25*, L249.

(19) Ammosov, M. V.; Delone, N. B.; Krainov, V. *P. Zh. Eksp. Theor. Fiz.* **1986**, *91*, 2008 (Engl. Trans.: *Sov. Phys. JETP* **1986**, *64*, 1191).

(20) Protopapas, M.; Keitel, C. H.; Knight, P. L. *Rep. Prog. Phys.* **1997**, *60*, 389.

(21) Fittinghoff, D. N.; Bolton, P. R.; Chang, B.; Kulander, K. C. *Phys. Rev. Lett.* **1992**, *69*, 2642.

(22) Corkum, P. B. *Phys. Rev. Lett.* **1993**, *71*, 1994.

(23) Kilic, H. S.; Ledingham, K. W. D.; Kosmidis, C.; McCanny, T.; Singhal, R. P.; Wang, S. L.; Smith, D. J.; Langley, A. J.; Shaikh, W. *J. Phys. Chem. A* **1997**, *101*, 817.

(24) Baumert, T.; Gerber, G. *Phys. Scr.* **1997**, *T72*, 53.

(25) Weinkauf, R.; Aicher, P.; Wesley, G.; Grotemeyer, J.; Schlag, E. W.; *J. Phys. Chem.* **1994**, *98*, 8381.

(26) DeWitt, M. J.; Levis, R. J. *J. Phys. Chem.* **1995**, *99*, 8670.

(27) Trushin, S. A.; Fuss, W.; Schikarski, T.; Schmid, W. E.; Kompa, K. L. *J. Chem. Phys.* **1997**, *106*, 9386.

(28) DeWitt, M. J.; Levis, R. J. *J. Chem. Phys.*, in press.

(29) DeWitt, M. J.; Levis, R. J. *Phys. Rev. Lett.* **1998**, *81*, 5101.

(30) Schilke, D. E.; Levis, R. J. *Rev. Sci. Instrum.* **1994**, *65*, 1903.

(31) DeWitt, M. J.; Peters, D. W.; Levis, R. J. *Chem. Phys.* **1997**, *218*, 211.

(32) Muller, H. G.; Agostini, P.; Petite, G. In *Atoms in Intense Laser Fields*; Gavrila, M., Ed.; Academic Press: New York, 1992.

(33) Gibson, G. N.; Dunne, G.; Berquist, K. J. *Phys. Rev. Lett.* **1998**, *81*, 2663.

(34) Freeman, R. R.; Bucksbaum, P. H.; *J. Phys. B: At. Mol. Phys.* **1991**, *24*, 325.

(35) Ilkov, F. A.; Decker, J. E.; Chin, S. L.; *J. Phys. B: At. Mol. Opt. Phys.* **1992**, *25*, 4005.

(36) Prall, B. S.; DeWitt, M. J.; Levis, R. J. *J. Chem. Phys.*, in press.

(37) Stewart, J. J. P. *J. Comput. Chem.* **1989**, *10*, 221.

(38) Billotto, R.; Levis, R. J. Manuscript in preparation.

(39) Zhang, J.; Lambropoulos, P. L. *J. Nonlinear Opt. Phys.* **1995**, *4*, 633.